

# BEAM-LOADING EFFECT IN THE NORMAL-CONDUCTING ILC POSITRON SOURCE PRE-ACCELERATOR

V. Paramonov\*, INR, Moscow, Russia, K. Floettmann, DESY, Hamburg, Germany

## Abstract

Significant positron bunch charge (several  $nC$ ) in the ILC Positron Source (PS) results in high pulse beam loading for normal-conducting accelerating structures in Positron Pre-Accelerator (PPA). Time interval between bunches ( $\sim 300ns$ ) is not negligibly small in comparison with accelerating structure time constant (rise time for Standing Wave (SW) or filling time for Traveling Wave (TW) options). As the result, beam loading effect has particularities both from stored energy acceleration regime and continuous beam loading one. Taking into account particular PPA beam structure, beam loading effect is estimated for the present ILC base line parameters, both for SW and TW PPA options. Possible solutions for beam loading compensation are discussed.

## INTRODUCTION

The concept of undulator based PS is chosen now as the base line in the ILC project development [1]. This PS scheme, considered in TESLA project [2], has the advantage of having a higher  $e^+$  yield and a better positron beam performance at the target. After the target and Adiabatic Matching Device (AMD) the positron beam should be captured and pre-accelerated in the normal conducting PPA linac. The main PPA purpose is to provide a maximum capture efficiency for the useful part of the incoming  $e^+$  beam with technically reasonable parameters of the linac.

The PPA scheme, investigated in [3], is shown in Fig. 1.

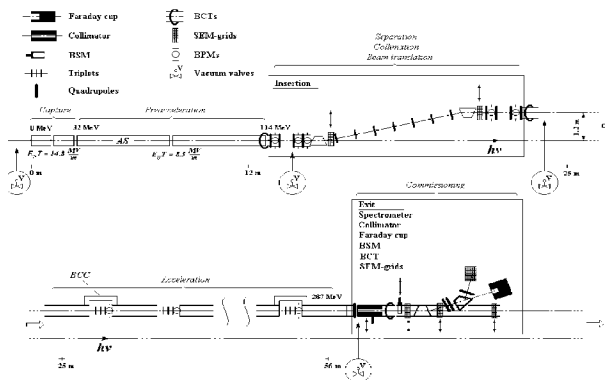


Figure 1: Investigated PPA scheme.

Functionally, proposed PPA consists of several parts - capture, pre-acceleration, beams separation, acceleration. In the ILC development such scheme can be optimized and

modified. Another decisions for PPA systems can be investigated. In this paper we consider one specific topic - beam loading effect in PPA normal conducting accelerating system. We use some general properties both of PPA beam and accelerating structures.

## BEAM PARAMETERS

After PPA capture part, beam pulse has a multi-bunch structure [3], shown in Fig. 2. Relative particles population in bunches depends on AMD field, accelerating gradient in PPA capture cavities and so on. We will use the main relationships. First  $e^+$  bunch contain main, dominated part of positrons. Second  $e^-$  bunch contain main, dominated part of electrons. Number of  $e^-$  in the second bunch is larger, than number of  $e^+$  in the first one. The first  $e^+$  bunch and the second  $e^-$  are separated by half rf wavelength and together extract energy from electric field.

The number of particles in the beam pulse has to be calcu-

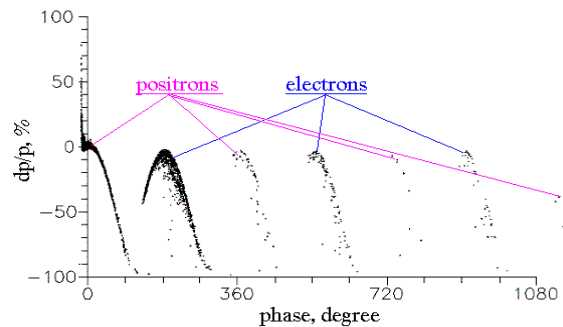


Figure 2: Multi bunch beam pulse structure.

lated starting from ILC IP point. Let us describe it, because intermediate multipliers define particle numbers in PPA parts and final beam loading effect. Should be  $2 \cdot 10^{10}e^+$  in ILC IP. Supposing no particle losses in the main linac, safety factor 1.5 is foreseen now for damping ring [1], resulting in  $\sim 3 \cdot 10^{10}e^+$ , required at the ring injection point. Not all  $e^+$  from the first bunch are in the range of the damping ring acceptance, and total number of positrons in the first bunch should be  $3.0 \cdot 10^{10} \cdot 1.5 \approx 4.5 \cdot 10^{10}$ . It is an estimation for the positrons number in the beam pulse after beam separations, with the charge  $q_1 = 7.2nC$ . Before separation, we have to take into account  $e^-$  from second bunch and total particles number in the beam pulse is  $\sim 4.5 \cdot 10^{10} \cdot 2.2 \approx 10^{11}$ , corresponding to the effective beam charge  $q_2 = 16nC$ . Time spacing between beam pulses is  $\delta t = 308ns$ , [1].

\*paramono@inr.ru

## ACCELERATING STRUCTURES

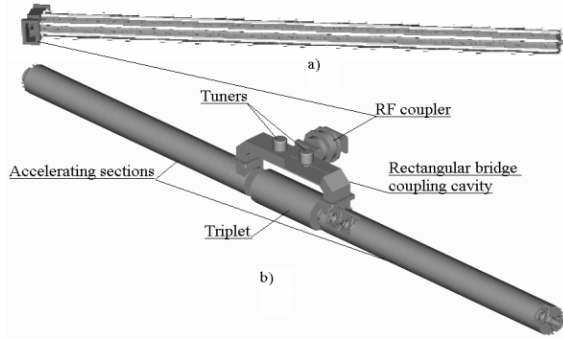


Figure 3: Proposed SW structure for PPA parts with solenoid (a) and triplet focusing (b).

Table 1: Parameters of proposed SW structure

Parameter	Unit	Value
Operating mode		$\pi$
$E_0T$	$\frac{MV}{m}$	8.5
$Z_e$	$\frac{MQ}{m}$	40.4
$Q_0$	(own)	21900
$\beta_g$	$\%c$	5.4
Rise-time $\tau_l$	$\mu s$	2.68
N cell (a)		37
N cell (b)		2x19
$P_{dis}$ (b)	MW	7.84

SW accelerating system, proposed for PPA [3], is based on compensated CDS structure (see, for example, [4]). Both pre-acceleration (with solenoid focusing) and acceleration (with triplet focusing) is suggested with the same accelerating gradient  $E_0T = 8.5 MV/m$ . Accelerating cells with the same shape and rf parameters, listed in Table 1, are foreseen for both options. For pre-acceleration we consider long cavities, Fig. 3a. RF input can be placed either at the cavity end, or in the middle. For main PPA part accelerating cavities are divided into two sections, Fig. 3b, jointed in resonant system by bridge cavities. It is required to place triplet between sections. Cavity rise-time  $\tau_l$  is

$$\tau_l = \frac{Q_0}{\pi f_0(1 + \eta)}, \quad (1)$$

where  $Q_0$  is the cells quality factor,  $f_0 = 1300 MHz$  and  $\eta \approx 1$  is the cavity - waveguide coupling factor. Parameters of TW structures we borrowed from reference [5]. In main rf parameters PPA SW and TW options were considered in [6], assuming phase advance  $\phi_0 = \frac{2\pi}{3}$  for TW structures. Increased phase advance in the proposal [5] leads to rf efficiency improvements for TW structures, simultaneously resulting in group velocity  $\beta_g$  reduction. Long TW section (Type 1) means for solenoid focusing,

shorter Type 2 one - for triplets. Parameters of the constant gradient TW structures [5] are reproduced in Table 2.

Table 2: Parameters of proposed [5] TW structures

Parameter	Type 1	Type 2
$\phi_0$	$\frac{3\pi}{4}$	$\frac{5\pi}{6}$
$E_0T, \frac{MV}{m}$	8.5	7.7
$Z_e, \frac{MQ}{m}$	50.05 $\div$ 39.68	46.34 $\div$ 36.37
$Q_0 \cdot 10^{-3}$	26.51 $\div$ 22.76	25.67 $\div$ 22.3
$\beta_g, \%c$	0.67 $\div$ 0.20	0.37 $\div$ 0.12
Cell number	50	23
Filling time $\tau_f$	3.6 $\mu s$	3.2 $\mu s$

## BEAM LOADING

In the beam loading calculations we follow the method, developed in [7]. Accelerating structure is considered as a part of transmission line with dispersion

$$\phi(\omega) = \phi_0 + \frac{d\omega}{c\beta_g} + \frac{d^2\phi(\omega)}{d\omega^2} + \dots \quad (2)$$

To describe the SW structures, this line part is shortened at one end and matched with rf input at another one. Transient is considered as a summation of forward and backward (reflected from shortened section end) waves, generated both by rf input and beam. For SW case  $\beta_g = const$  along the structure.

The line part, matched at both section ends, represents TW structure. This case we have no reflected waves from the section ends, but  $\beta_g$  is variable along the section.

The dispersion description (2) we restrict with  $\phi_0$  and linear (in  $d\omega$ ) terms, which describe average picture of wave propagation. The higher order terms describe details of propagating wave front, both front smearing and hits at the front. It strongly complicate calculations, but not important for average effect values fro relatively short structures.

Time of the beam flight  $t_{fl}$  through the structure is  $\approx 19t_{rf} = 14ns$  for long sections and  $t_{fl} = 9t_{rf} = 7ns$  for short ones, where  $t_{rf} = 0.77ns$  - is the rf period. Because  $t_{fl} \ll \delta t \ll \tau_l \approx \tau_f$ , we can consider beam flight through the section and energy extraction from rf field as an instant event, synchronous for all structure cells.

Passing through the accelerating structure, the beam pulse takes out from the stored field energy  $W_c$  the part  $W_b = E_0TLq$ , leading to an accelerating field reduction [8]:

$$\delta E \approx -\frac{\pi f_0 q Z_e}{Q_0}. \quad (3)$$

This estimation is common both for SW and TW structures. For structures parameters, listed in Table 1 and Table 2  $W_b \approx 1.27\%W_c$ ,  $\delta E \approx 0.054 \frac{MV}{m}$  for  $q = q_1 = 7.2nC$  and  $W_b \approx 2.84\%W_c$ ,  $\delta E \approx 0.12 \frac{MV}{m}$  for  $q = q_2 = 16.0nC$ , respectively. But field recovery pattern is quite different for SW and TW options.

In the compensated SW structure the time of traveling wave propagation  $\tau_{tr}$  from rf input point to the section shortened end is  $\tau_{tr} = \frac{L}{c\beta_g} \approx 260ns$  for long SW sections (Fig. 3a) and  $\tau_{tr} \approx 130ns$  for shorter ones, Fig. 3b. As one can see, time between beam pulses is sufficient at least for one traveling wave pass through the SW section, leading to partial recovery of rf field value. For total field recovery

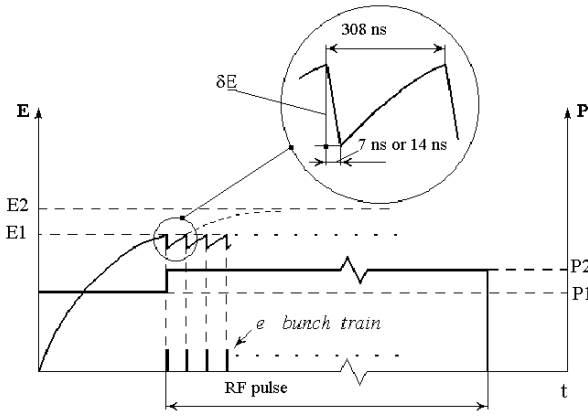


Figure 4: The 'saw-tooth' field amplitude in SW structures.

several wave passes are required and field recovery process in compensated SW structure is step-like (in time) [7],[3], but with envelope  $\sim (1 - e^{-\frac{t}{\tau_i}})$ . With  $\tau_{tr} \leq \delta t$  all cells in SW structure are approximately at the same conditions with respect field value. Schematically the simplified time diagram for the accelerating field amplitude is shown in Fig. 4. Suppose, the designed field amplitude in the structure is  $E_1$ , corresponding to the rf input power  $P_1$ . After first beam pulse there is field reduction at  $\delta E$  value, (3). Because  $\delta t \sim 308ns \ll 3\tau_l \sim 7\mu s$ , the field can not be restored for  $E_1$  value, without additional rf power, to the time of next beam pulse. The new power set-up point  $P_2$  should be established to have another field amplitude  $E_2$  at  $t \rightarrow \infty$  with the purpose to have  $E_1$  for the next beam pulse. Considering field amplitude behavior and rf power balance, one can find:

$$P_2 = P_1 \left( 1 + \frac{\delta E}{E_1} \frac{\exp(-\frac{\delta t}{\tau_l})}{1 - \exp(-\frac{\delta t}{\tau_l})} \right)^2, \quad (4)$$

Values of additional rf power required  $\delta P = P_2 - P_1$  are  $\approx 0.12P_1$  and  $\approx 0.25P_1$  for beam pulse charges  $q = q_1 = 7.2nC$  and  $q = q_2 = 16nC$ , respectively.

For TW structure the field recovery takes place only due to forward wave from rf input. The field distributions along TW structures in steady-state regime before beam pulse entering the sections are shown in Fig. 5. To explain this step-like behavior, let us divide TW sections in intervals  $z_1, z_2, \dots, z_n, \dots$  with the length, in which traveling wave propagates at a time  $\delta t$ . In constant gradient TW structure  $\beta_g$  decreases with cell number and  $z_n > z_{n+1}$ . At time interval  $\delta t$  the direct wave from rf input will fill the first interval  $z_1$  and recover field to unloaded value. But

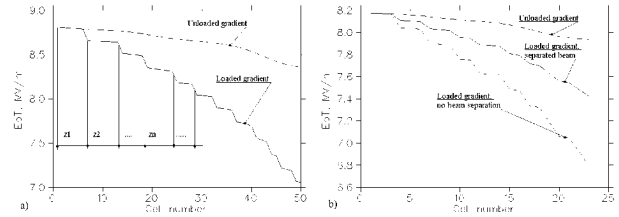


Figure 5: Steady-state field amplitude distribution along TW structures Type 1 (a) and Type 2 (b) before beam pulse.

next interval  $z_2$  will be filled with the wave, which was attenuated with previous beam pulse and its amplitude was decreased at  $\delta E$ . And so on, interval  $z_n$  will be filled with wave, which was attenuated with  $(n - 1)$  previous beam pulses and its amplitude was decreased properly, at  $\approx (n - 1)\delta E$ . Comparing  $\tau_f$  from Table 2 and  $\delta t$  one can see, that at TW structure length there is 10 or 11 intervals  $z_n$  and field distribution has 10 or 11 steps. As it is usual for TW structures, loaded  $E_0T$  value is less than unloaded one. Relative reduction of average  $E_0T$  value for TW structure Type 1 is 6.1%,  $q = q_2 = 16.0nC$ . For Type 2 structure the same values are 5.6%,  $q = q_2 = 16.0nC$  and 2.5%,  $q = q_1 = 7.2nC$  for non-separated and separated beam, respectively.

Both for SW and TW structures, additional rf power is required to compensate beam loading effect. The value of beam loading, definitely, depends on beam pulse charge. From the point of view of rf power saving, beam separation in PPA is preferable as early, as it is reasonable from positron dynamics conditions.

## REFERENCES

- [1] ILC base line parameters. <http://www.linearcollider.org>
- [2] TESLA Technical Design Report, DESY, Hamburg, 2001.
- [3] K. Flottmann, V. Paramonov (ed.) Conceptual design of a positron injector for the TESLA linear collider. TESLA 99-14, TESLA 2000-12, Hamburg, DESY.
- [4] V. Paramonov et al., The PITZ Booster Cavity A Prototype for the ILC PS Cavities. PAC 2005, p. 1030, 2005.
- [5] J.W. Wang, et al., Studies of Room Temperature Structures for the ILC Positron Source. PAC 2005, p. 2827, 2005. Preliminary studies of rf structures for ILC Positron Source. Workshop on PS for ILC, Daresbury, April 11-13, 2005.
- [6] V. Moiseev et al., Comparison of SW and TW operations for a Positron Pre-Accelerator in the TESLA Linear Collider. EPAC2000, p. 842, 2000.
- [7] M.F.Vorogushin, V.N. Malyshev. RF systems of resonant accelerators for applied purposes. Energoatomizdat, Moscow, 1989, (in Russian)
- [8] P. Wilson, Transient beam loading in electron-positron storage rings, CERN-ISR-TH/78-23, 1978.